Self-assembly of Pluronic F127-Diacrylate in Ethylammonium Nitrate: structure, rheology and ionic conductivity before and after photo-crosslinking (Supporting Information)

Carlos R. López-Barrón, Ru Chen, Norman J. Wagner, Peter J. Beltramo

Scattering Models. Two models were used to fit the SANS data. For the low concentration solutions, a *spherical core-shell model* was used. This model calculates the form factor for non-interacting polydisperse spherical particles having a core-shell structure with radius R_s, core radius R_c, and shell thickness $T_s = R_s - R_c$. The functional form is given as:[1, 2]

$$P(q) = \frac{scale}{V_s}\left[\frac{3V_c(\rho_c - \rho_s)\, j_1(qR_c)}{qR_c} + \frac{3V_s(\rho_s - \rho_{solv})\, j_1(qR_s)}{qR_s}\right]^2 \quad (1)$$

where ρ_c, ρ_s and ρ_{solv} are the scattering length densities (SLDs) of the core, shell and solvent, respectively, $j_1(x) = (\sin x - x\cos x)/x^2$, and $V_i = 4\pi R_i^3/3$. The quantity in the braces in Equation 1 is equal to $< f * f >$, where f is the single particle scattering amplitude, appropriately averaged over the Schulz distribution of radii.[3] The spherical particles have a constant shell thickness and polydisperse core with polydispersity given as $PDI \equiv \sigma / R_c$, where σ^2 is the variance of the distribution. The *scale* factor can be set equal to the particle volume fraction to obtain the scattering intensity per unit volume. The fittings were performed using the IGOR macros available from NCNR. [2] Three parameters were fixed for the fitting, namely, $\rho_c = 3.43\times10^{-7}$ Å^{-2}, $\rho_s = 3.87\times10^{-6}$ Å^{-2} and the *scale* factor, whose value was the corresponding volume fraction. The parameters R_c, T_s, PDI and ρ_{solv} were varied during the fitting.

The second scattering model used for the concentrated solutions is the *FCC lattice model with paracrystalline distortion*. This model considers monodisperse spherical particles with radius R, volume V_p, and volume fraction ϕ, ordered in an infinitely large FCC cubic lattice with isotropic paracrystalline distortion. The scattering intensity is given as:

$$I(q) = \frac{\phi}{V_p} V_{lattice} P(q) Z(q) \tag{2}$$

where $V_{lattice}$ is the occupied volume of the lattice, $P(q)$ is the normalized sphere form factor given as

$$P(q) = \left[\frac{3}{qR} \left(\frac{\sin(qR)}{(qR)^2} - \frac{\cos(qR)}{qR} \right) \right]^2 \tag{3}$$

and $Z(q)$ is the paracrystalline structure factor for FCC structures, which are calculated with equation (1) in Ref. [4] and equations (23)-(25) in Ref. [5].

Supplementary SANS data analysis. We used SANS measurements to elucidate the microstructure of (non-crosslinked) FDA/dEAN solutions. Figure S1(a) shows SANS profiles of a 5 wt% FDA/dEAN solution at different temperatures. At 30 °C, the typical scattering profile corresponding to the form factor of spherical objects is observed. These data is well fitted with the core-shell model (solid line), described above. The observed scattering upturn dominates the scattering profile at lower temperatures (25 °C and 15 °C). However the scattering corresponding to the q-values > 0.02Å^{-1} can still be fitted to the core-shell model, as indicated by the solid lines. The parameters used for the fitting are given in Table S1. A comparison of the scattering from 5 wt% solutions of non-functionalized F127 and functionalized F127 (FDA) in dEAN is given in Figure S1(b). The size of the micelles for both solutions are practically the same

(see Table S1), which indicates that the presence of the acrylate groups at the ends of the block copolymer have no effect on the micelle formation.

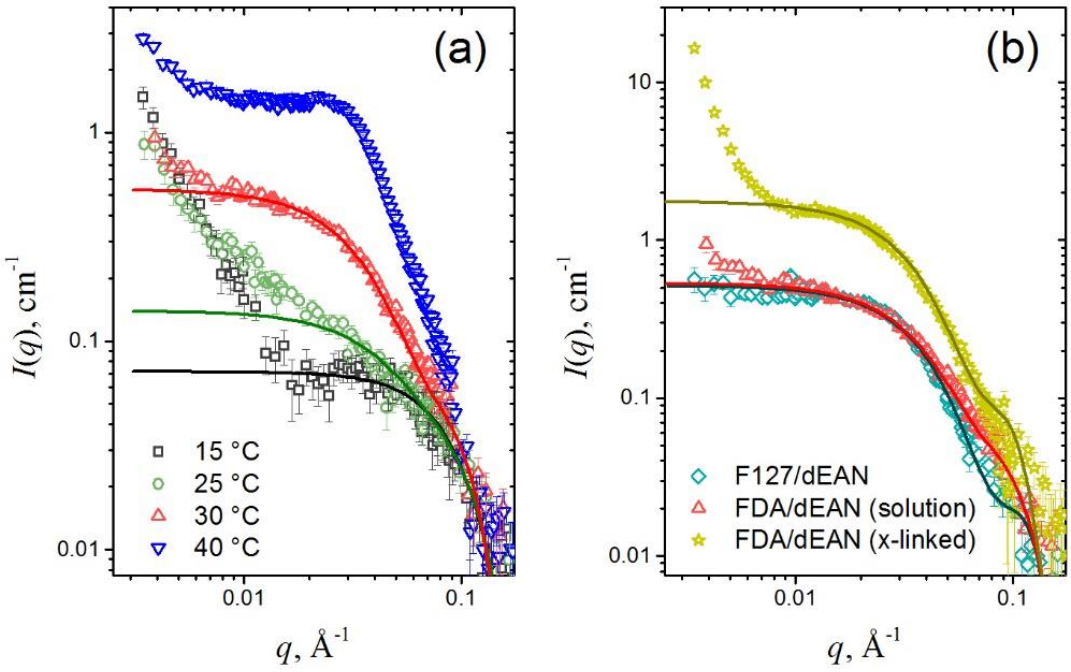

Figure S1. (a) SANS profiles of a 5 wt % FDA/dEAN solutions measured at the indicated temperatures. (b) SANS profiles measured at 30 °C of a 5 wt % F127/dEAN and a 5 wt% FDA/dEAN solution before and after crosslinking. Solid lines are best fits to the core−shell model described in the text.

Table S1 gives the aggregation number, N_{agg}, the volume of the corona (shell), V_s, the volume of the dry corona, $V_{\text{s-dry}}$, and the volume fraction of dEAN in the corona, $\phi_{\text{dEAN-in-corona}}$, which are calculated using R_c, T_s, the bulk densities of PPO, ρ_{PPO}, and PEO, ρ_{PEO}, the molecular weights of the PPO center block, M_{PPO}, and the PEO end blocks, M_{PEO}, and the Avogadro's number, N_A, as

$$N_{\text{agg}} = \frac{4}{3}\pi R_c^{\,3}\rho_{\text{PPO}}\frac{N_A}{M_{\text{PPO}}}, \qquad (4)$$

$$V_s = \frac{4}{3}\pi\left[\left(R_c + T_s\right)^3 - R_c^3\right], \quad (5)$$

$$V_{\text{s-dry}} = \frac{N_{\text{agg}}}{N_A}\frac{M_{\text{PEO}}}{\rho_{\text{PEO}}}, \text{ and} \quad (6)$$

$$\phi_{\text{dEAN-in-corona}} = \frac{V_s - V_{\text{s-dry}}}{V_s}. \quad (7)$$

Table S1. Geometrical parameters of F127/dEAN and FDA/dEAN micelles, as determined by SANS.

Sample	T, °C	soln/x-linked	R_c nm	T_s nm	PDI	N_{agg}	$V_s \times 10^3$ nm^3	$V_{\text{s-dry}} \times 10^2$ nm^3	$\varphi_{\text{dEAN-in-corona}}$
5 wt% FDA/dEAN	15	solution	2.1±0.06	4.7±0.36	0.27±0.07	5.09	1.23	0.71	0.942
		x-linked	2.2±0.03	5.5±0.06	0.31±0.01	6.77	1.87	0.94	0.950
	25	solution	2.1±0.05	4.6±0.21	0.15±0.01	5.89	1.22	0.82	0.933
		x-linked	2.3±0.05	5.2±0.05	0.09±0.001	7.74	1.72	1.07	0.937
	30	solution	2.4±0.03	5.0±0.09	0.04±0.002	8.79	1.64	1.22	0.926
		x-linked	3.0±0.05	5.5±0.07	0.02±0.005	15.5	2.95	2.15	0.927
5 wt% F127/dEAN	30	solution	2.5±0.01	4.8±0.01	.01±0.001	9.94	1.56	1.38	0.912
10 wt% FDA/dEAN	15	solution	1.9±0.20	6.3±0.7	0.15±0.03	5.89	1.40	0.82	0.942
		x-linked	2.2±0.09	5.5±0.22	0.11±0.006	6.77	1.87	0.94	0.950

The core-shell model used to obtain the fitting data given in Table S1 assume that the micelle is composed of a compact PPO core without dEAN, a solvated PEO shell, and that all the polymer chains in the micelle are non-interacting. It is also assumed constant SLD distribution at micelle core, shell, and solvent regime. Based on the closed association model, micellization is a cooperative process, where numerous unimers are in a dynamic equilibrium between micelles at concentration above critical micelle concentration (CMC).

Hence, both free polymer chains in the solvent and polymer chains in the micelles are needed to be accounted for in the mass balance. To provide accurate quantitative analysis on the fitting results, $I(0)$ is used to constrain the *scale* factor, ϕ_{total}, and mass balance is used to constrain ρ_s and ρ_{solv}. $I(0)$ is given as

$$I(0) = \frac{\left[\frac{4}{3}\pi(\rho_c - \rho_{solv})R_c^{\,3} + \frac{4}{3}\pi T_s(\rho_s - \rho_{solv})(3R_c^{\,2} + 3R_cT_s + T_s^{\,2})\right]^2}{\frac{4}{3}\pi(R_c + T_s)^3}\phi_{\text{total}} \times 10^8 \tag{8}$$

Species mass balance for F127 (or FDA) gives

$$N_{\text{F127-total-chains}} = N_{\text{F127-chains-in-solvent}} + N_{\text{agg}}\frac{\phi_{\text{total}}}{\frac{4}{3}\pi(R_c + T_s)^3} \tag{9}$$

In this framework, N_{agg} accounts for the volume fraction of dEAN in the micelle core, $\phi_{\text{dEAN-in-core}}$, and therefore it is given as

$$N_{\text{agg}} = (1-\phi_{\text{dEAN-in-core}})\frac{4}{3}\pi R_c^{\,3}\frac{\rho_{\text{PPO}}N_A}{M_{\text{PPO}}} \tag{10}$$

Using known SLD of dEAN and F127, as well as the volume fraction for F127 chains in the solvent, $\phi_{\text{F127-in-solvent}}$, the SLD of the micelle core, ρ_c, and of the solvent, ρ_{solv}, are obtained via mass balance as

$$\rho_c = \phi_{dEAN-in-core}\rho_{dEAN} + (1-\phi_{dEAN-in-core})\rho_{PPO} \tag{11}$$

$$\rho_{solv} = \phi_{\text{F127-in-solvent}}\rho_{\text{F127}} + (1-\phi_{\text{F127-in-solvent}})\rho_{\text{dEAN}} \tag{12}$$

New fittings are obtained using the core-shell model combined with the species mass balances given by Equations (8)-(12). Fitting results for 5 wt% F127/dEAN at 25 °C and 5 wt% FDA/dEAN solution and

cross-linked samples at 15, 25 and 30 °C are shown in Table S2. The fitting results provide evidence that that F127 and FDA micelles formed in dEAN have nearly dry micelle core (with dEAN volume fraction in the core less than 0.1).

Table S2. Geometrical parameters of F127/dEAN and FDA/dEAN micelles, as determined by SANS and fittings to the modified core-shell model including species mass balances given in Equations (8) to (12).

Sample	T, °C	soln/ x-linked	R_c nm	T_s nm	PDI	N_{agg}	$V_s \times 10^3$ nm^3	$V_{s\text{-dry}} \times 10^2$ nm^3	$\phi_{dEAN\text{-in-corona}}$	$\phi_{dEAN\text{-in-core}}$
5 wt% FDA/dEAN	15	solution	0.96±0.1	2.1±0.1	0.03±0.002	6.84	2.31	0.98	0.96	0.03
		x-linked	2.3±0.27	9.4±0.60	0.04± 0.002	7.21	6.53	1.01	0.98	0.014
	25	solution	1.4±0.59	3.2±0.91	0.09±0.002	4.79	1.78	0.46	0.98	0.02
		x-linked	2.1±0.63	6.3±0.45	0.02±0.01	5.49	2.45	0.77	0.97	0.053
	30	solution	1.7±0.38	4.4±0.58	0.04±0.001	3.11	0.94	0.44	0.92	0.020
		x-linked	2.1±0.31	6.1±0.22	0.08± 0.001	5.43	2.31	0.76	0.97	0.099
5 wt% F127/dEAN	30	solution	1.3±0.28	5.4±0.27	0.03±0.001	1.48	1.56	1.38	0.912	0.0067

Figure S2 shows that the intermicellar scattering peak is more pronounced at higher polymers concentrations and higher temperatures for compositions up to 20 wt%. The characteristic intermicellar distance, calculated as $d = 2\pi/q^*$, where q^* is the position of the main scattering peak in Figure S2, is plotted as a function of temperature in Figure S3. As expected, d decreases with composition, but no change with temperature is observed in the solutions before and after crosslinking.

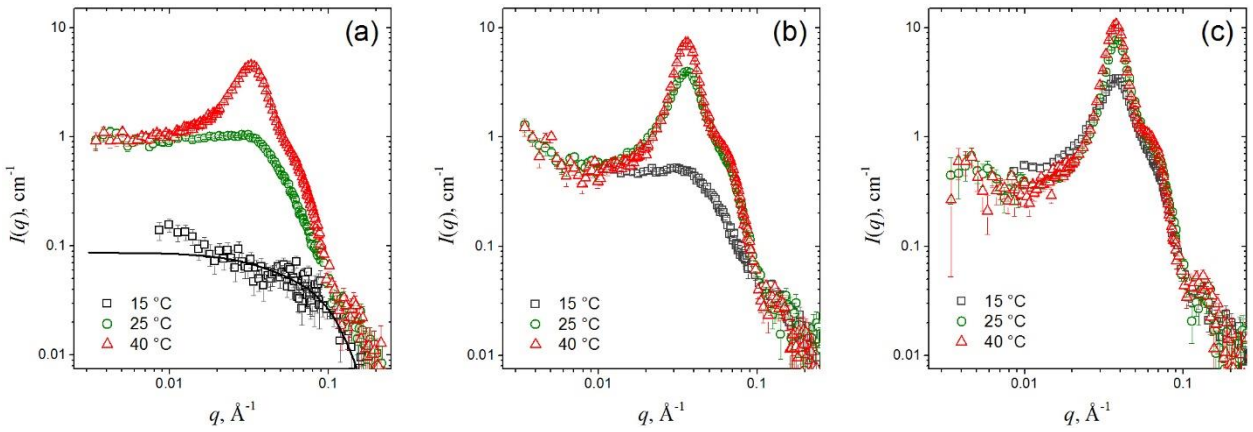

Figure S2. SANS profiles of (a) 10 wt%, (b) 15 wt% and (c) 20 w% FDA/dEAN solutions measured at the indicated temperatures. Solid line in (a) is the best fit to the core−shell model described in the text.

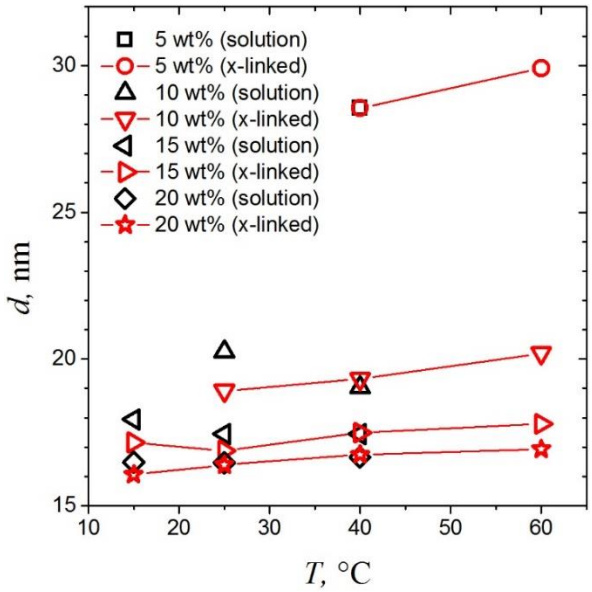

Figure S3. Inter-micellar distance as a function of temperature for FDA solutions before and after crosslinking.

Table S3 shows the geometrical parameters of the FCC lattice for the 24 wt% FDA/dEAN ion gels along with the recently reported values for the 24 wt% F127/dEAN gel.[6] The FCC model provides values of

sphere radius, R, and the nearest-neighbor separation, D. Using these two parameters, we can calculate the occupied volume fraction of the lattice as $\phi_{\text{latt}} = 16\pi/3\sqrt{8} \times (R/D)^3$.[4, 5]

By comparing the values of the lattice parameters for the F127/dEAN and the FDA/dEAN gels, it is evident that the acrylation of the triblock end groups has no effect on the crystalline structure of these gels. The small increase in micelle radius with temperature is in agreement with the increase in aggregation number observed in the more dilute solutions (Table S1), which result from the lower solubility of the triblock copolymer. This also explains the slight increase in ϕ_{latt} with temperature.

Table S3. Lattice parameters of cubic unit cells in 24 wt% F127/dEAN and 24 wt% FDA/dEAN gels, before and after crosslinking.

Sample	Temperature	R, nm	D, nm	ϕ_{latt}
F127/dEAN[a]	40	4.90 ± 0.005	28.0 ± 0.01	0.032
FDA/dEAN (solution)	25	4.67± 0.004	27.9± 0.01	0.027
FDA/dEAN (solution)	40	4.81± 0.004	28.1± 0.001	0.030
FDA/dEAN (x-linked at 15 °C)	15	4.59± 0.004	27.2± 0.01	0.028
FDA/dEAN (x-linked at 15 °C)	40	4.87± 0.004	28.3± 0.01	0.030
FDA/dEAN (x-linked at 40 °C)	15	4.56± 0.005	27.9± 0.01	0.026
FDA/dEAN (x-linked at 40 °C)	25	4.71± 0.005	28.2± 0.01	0.028
FDA/dEAN (x-linked at 40 °C)	40	4.84± 0.005	28.5± 0.01	0.029

[a]The data for the 24 wt% F127/dEAN are taken from López-Barrón et al.[6]

Dielectric spectroscopy measurements

The frequency and temperature dependence of the complex permittivity and conductivity of deuterated ethylammonium nitrate (dEAN) and FDA/dEAN solutions before/after crosslinking is shown in Figure S4-S8. At low frequencies, the effects of electrode polarization (EP) are clearly seen in the ω^{-2} dependence of ε'. Qualitatively, this effect occurs at lower frequencies as FDA is added to the system. To quantify this effect, we note that the onset of EP in the permittivity is a function of the spacer thickness, *h*, ion diffusion coefficient, *D*, and debye length, κ^{-1}, by[7]

$$\omega_{EP} \sim \frac{\kappa^{3/2} D}{h^{1/2}} \quad . \tag{13}$$

The ion diffusion coefficient and spacer thickness are constant between our experiments, and the Debye length is proportional to the concentration of ions in the system by

$$\kappa = [I]^{1/2} \quad . \tag{14}$$

Although we do not know exactly value of the Debye length in the samples, dEAN is the primary source of ions and therefore we expect the onset of EP to decrease by $[I]^{3/4}$ as FDA is added to the system and the concentration of dEAN decreases. To check this, we plot the frequency at which $\varepsilon' = 10^4$ as a function of dEAN concentration in Figure S9. The values are scaled by the frequency at which $\varepsilon' = 10^4$ for the pure dEAN samples. $\varepsilon' = 10^4$ was chosen to have a consistent metric between the different samples, as it is well within the ω^{-2} regime of the permittivity where the EP effects dominate and there is little curvature in the spectra. From Figure S9, we observe that EP occurs at a lower frequency than expected by just considering the concentration of dEAN, as we did above. A possible explanation for this is that ion binding to the micelle corona hinders dEAN ion transport. As the temperature increases, this effect is weakened (the scaled values increase closer to the expected values), which correlates with the subtle effect

noted in the manuscript that the difference in conductivity between the neat dEAN and mixtures decreases with temperature. Lastly, crosslinking also partially mitigates this effect, agreeing with the slight increase in conductivity, to imply that the ion binding is reduced.

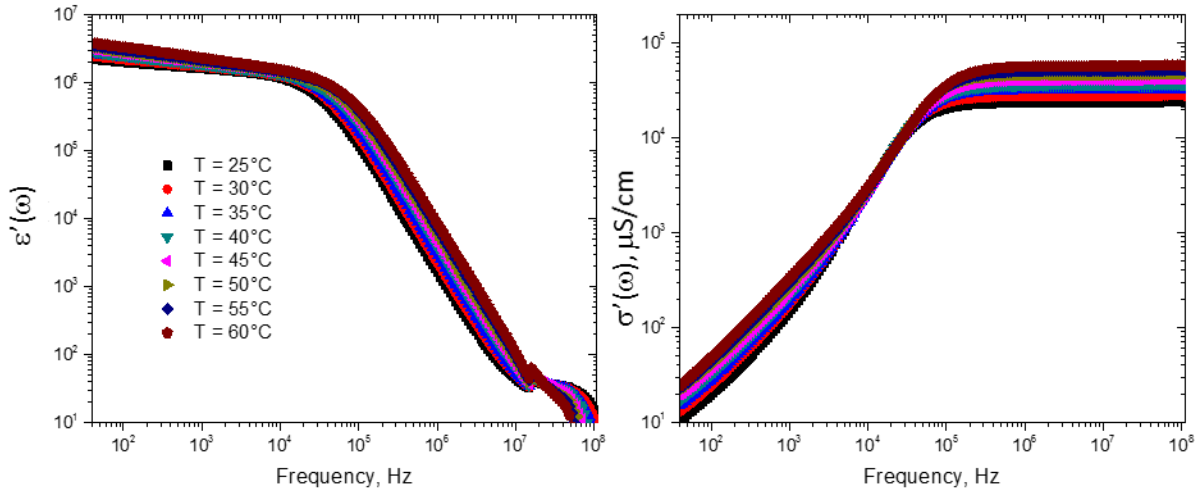

Figure S4. Complex dielectric permittivity and conductivity of dEAN as a function of frequency at indicated temperatures.

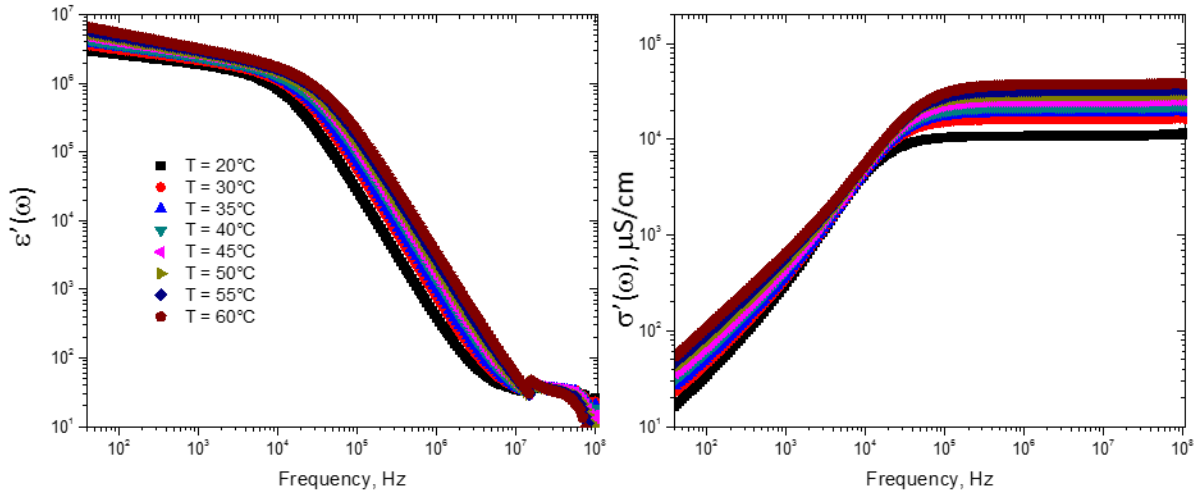

Figure S5. Complex dielectric permittivity and conductivity of 15 wt% uncross-linked F127DA as a function of frequency at indicated temperatures.

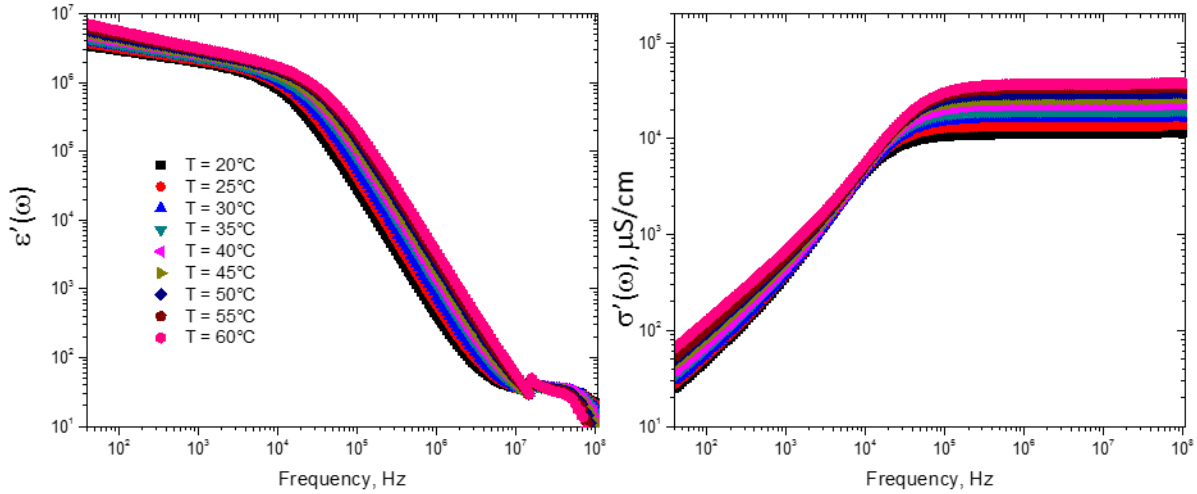

Figure S6. Complex dielectric permittivity and conductivity of 15 wt% cross-linked F127DA as a function of frequency at indicated temperatures.

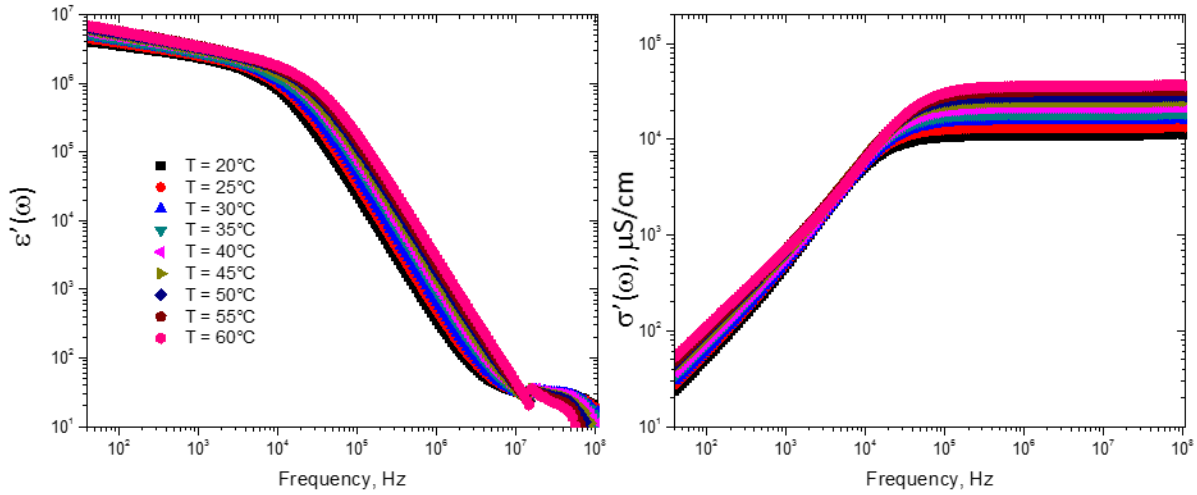

Figure S7. Complex dielectric permittivity and conductivity of 22.5 wt% uncross-linked F127DA as a function of frequency at indicated temperatures.

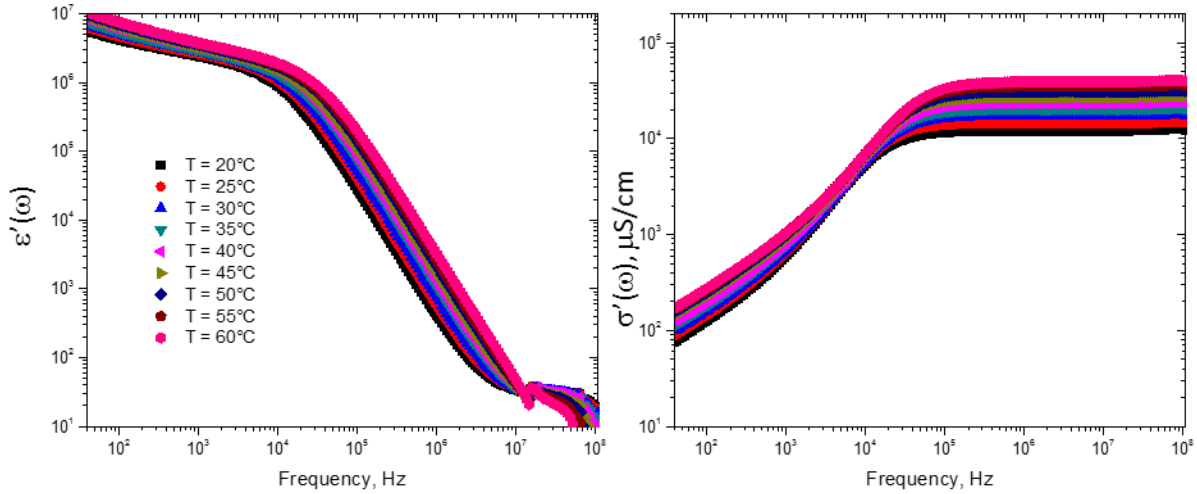

Figure S8. Complex dielectric permittivity and conductivity of 22.5 wt% cross-linked F127DA as a function of frequency at indicated temperatures.

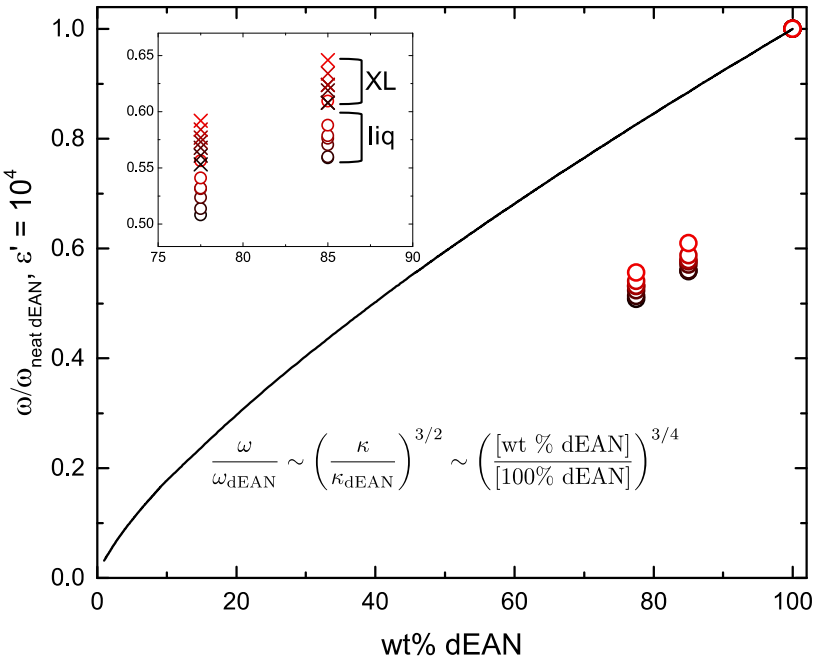

Figure S9. Frequency at which $\varepsilon' = 10^4$ as a function of dEAN concentration and temperature. The temperature increases from 30°C to 60°C in 5° increments from black to red. The line indicates the expected decrease due to concentration effects only. The inset is a zoomed in view of the area of interest which also shows the data for crosslinked samples.

References

1. Guinier, A.; Fournet, G. *Small-angle scattering of X-rays;* Wiley: New York, 1955; , pp 268.

2. Kline, S. R. *J. Appl. Cryst.* **2006**, *6*, 895-900.

3. Bartlett, P.; Ottewill, R. H. *J. Chem. Phys.* **1992**, *4*, 3306-3318.

4. Matsuoka, H.; Tanaka, H.; Iizuka, N.; Hashimoto, T.; Ise, N. *Phys. Rev. B* **1990**, 3854-3856.

5. Matsuoka, H.; Tanaka, H.; Hashimoto, T.; Ise, N. *Phys. Rev. B* **1987**, 1754-1765.

6. López-Barrón, C. R.; Li, D.; Wagner, N. J.; Caplan, J. L. *Macromolecules* **2014**, *21*, 7484-7495.

7. Hollingsworth, A. D.; Saville, D. A. *J. Colloid Interface Sci.* **2003**, *1*, 65-76.